Int. J. Industrial. Model. chem. 2025; 16(1) 1-11

International Journal of Industrial Chemistry (IJIC)

https://doi.org/10.57647/j.ijic.2025.1602.11

Improved Photocatalytic Degradation of Methylene Blue: Synergistic Effects of Cobalt Sulfide-Silver Nanocomposites Under Visible Light Irradiation

Zahra Alinezhad, Reza Fazaeli*, Hamidreza Moghadamzadeh, Mehdi Ardjmand, Nahid Raoufi

Department of Chemical Engineering, South Tehran Branch, Islamic Azad University, Tehran, Iran

***Corresponding author:** r_fazaeli@azad.ac.ir

Original Research

Received:
7 December 2024

Revised:
11 March 2025

Accepted:
24 March 2025

Published in Issue:
30 June 2025

Abstract

In the present study, the investigation into the photodegradation of methylene blue dye was conducted utilizing synthesized cobalt sulfide (CoS), silver nanoparticles, and a silver-cobalt sulfide (Ag/CoS) composite, all subjected to visible light irradiation. The morphological characteristics were examined through XRD, SEM, and Mott-Schottky analyses. XRD analysis revealed a hexagonal structure for cobalt sulfide, while the composite displayed rectangular and polygonal forms. Mott-Schottky analysis showed that the presence of a p-n heterojunction, with the semiconductor flat band potentials measured at -1.2 V for the n-type and 1.5 V for the p-type. The composite's bandgap was identified as 2.4 eV through DRS analysis. Various factors, including temperature, pH, and the percentage of silver doping, significantly influenced the degradation rate. While both Cobalt Sulfide and Ag alone could degrade methylene blue, the silver-cobalt sulfide composite demonstrated superior performance, achieving a 92% degradation rate. The Sips and Khan models demonstrated the superior alignment with the degradation data, exhibiting the most elevated correlation coefficients and the minimal error functions (0.008, 0.057) and (0.01, 0.078), respectively.

Keywords: Methylene blue, Photocatalyst, Silver nanoprticles, Mott–Schottky, p-n Heterojunction, Cobalt sulfide

Cite this article: Alinezhad Z., Fazaeli R., Moghadamzadeh H., Ardjmand M., Raoufi N. (2025). Improved Photocatalytic Degradation of Methylene Blue: Synergistic Effects of Cobalt Sulfide-Silver Nanocomposites Under Visible Light Irradiation, *International Journal of Industrial Chemistry; 16(2):* 1-11. https://doi.org/10.57647/j.ijic.2025.1602.11

1. Introduction

Water pollution remains a critical issue as it directly impacts both living organisms and the environment [1,2]. The presence of organic pollutants in water is a major concern for the water industry, environmental advocates, and the public, given its detrimental effects on human, animal, and wildlife health, including pets, birds, and aquatic species. One of the primary environmental pollutants is textile wastewater. Dyes such as methylene blue, which possess complex aromatic molecular structures, are highly stable and resistant to degradation, making them significant contributors to water pollution and harmful to living organisms [3,4,5]. To address this, various methods, including filtration [6], chemical oxidation[7], coagulation [8], and biological treatment [9], have been explored for removing organic contaminants. Among the available physical, chemical, and biological wastewater treatment techniques, heterogeneous

photocatalysis stands out as a cost-effective approach due to its rapid oxidation capabilities without forming polycyclic byproducts and its effectiveness at low pollutant concentrations [10,11,12].

Recently, cobalt sulfides characterized by various chemical compositions (CoS2, CoS, Co9S8, Co3S4, Co1−xSx) [13-21] have attracted significant scholarly interest due to their extensive array of applications, including their utility as electrocatalysts in oxygen evolution reactions, as electrode materials in rechargeable lithium [22-24] and alkaline battery systems, as magnetic materials, in solar cells [25-30], for hydrogen storage, and as photocatalysts under visible light conditions. Prior research on cobalt sulfide synthesis and composites for degrading dyes like methylene blue highlights its potential as a highly efficient catalyst[31-36]. Furthermore, semiconductor photocatalysts doped with silver nanoparticles have proven effective for breaking down pollutants. The addition of silver nanoparticles significantly enhances pollutant removal and improves decontamination in aqueous environments due to silver's high plasmonic properties and its strong interaction with light, as well as shifting the spectral absorption range toward the visible light spectrum in silver-based composites[37-43].

A heterojunction refers to the interface between two dissimilar semiconductor materials, which have different bandgaps compared to homojunctions. Combining different semiconductor layers forms a heterogeneous structure[44-47]. In p-n heterojunctions, the contact between two semiconductors creates a junction that facilitates the transport of electrons and holes in opposite directions. These semiconductors are categorized as type p or n based on their donor and acceptor properties. In the present study, CoS nanoparticles were synthesized, and methylene blue degradation was performed in a tube reactor using visible light. Silver nanoparticles were also synthesized, each degrading a portion of the pollutant individually. However, when silver was deposited onto cobalt sulfide, a highly efficient composite was formed, significantly increasing the degradation rate. Various tests on the composite identified optimal conditions for temperature, pH, and silver dopant percentage.

2. Experimental Section

$Co(NO_3)_2 \cdot 6H_2O$, surfactants including acetyl trimethyl ammonium bromide ($C_{16}H_{33}N(CH_3)_3Br$), sodium dodecyl sulfate ($NaC_{12}H_{25}SO_4$), polyethylene glycol ($C_{2n}H_{4n+2}O_{n+1}$), silver nitrate ($AgNO_3$), glucose ($C_6H_{12}O_6$), methylene blue ($C_{16}H_{18}N_3SCl$), and ethanol (C_2H_5OH) were obtained from Sigma-Aldrich Co. These chemicals were used as received without any further purification.

3. Photoreactor Design

The photoreactor used in this experiment is a batch-type system, consisting of a cylindrical Pyrex tube. A white LED strip, 7 meters in length, is wrapped around the tube. The system operates at 220 volts and 50 watts, ensuring uniform light exposure across the sample. A magnetic stirrer was employed to keep the sample continuously agitated. Fig 1 provides a schematic of the photoreactor setup.

Figure 1. Photocatalytic Reactor

4. Synthesis of CoS

1 mole of cobalt nitrate, alongside 1 mole of thiourea, was introduced into 20 ml of deionized water, in conjunction with 10 ml of polyethylene glycol and surfactants, specifically SDS at a concentration of 0.02 g and CTAB at a concentration of 0.003 g, and subsequently subjected to a stirrer heater for a duration of 4 hours to facilitate the transition to a black precipitate. Thereafter, the resultant precipitate underwent multiple centrifugation cycles and was rinsed with ethanol+deionized water solution before being placed in an oven maintained at 220 oC for the purpose of desiccation. The X-ray diffraction (XRD) analysis conclusively identified the presence of cobalt sulfide. (Fig 2)

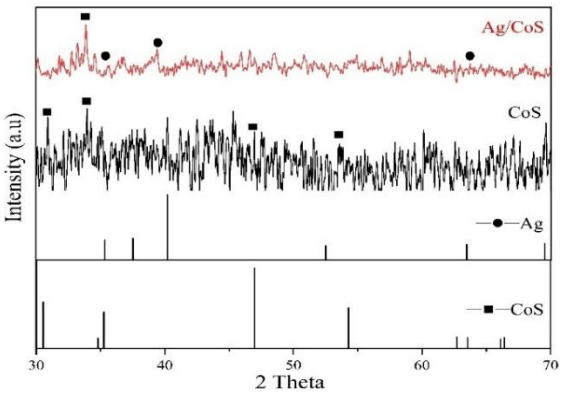

Figure 2. Diffraction pattern for CoS and Ag/CoS

5. Synthesis of silver

to 1.0 g of synthesized CoS, 12 ml of silver nitrate of 2000 mg/L were added with an emitter and placed on the stirrer for one hour. Then it was placed in an oven at 160 °C to ensure complete solvent evaporation and to enhance surface interaction between cobalt sulfide (CoS) and silver ions (Ag^{+}), after drying, it was washed ith ethanol and deionized water and put back in the oven. It was calcined at 500 oC for 3 hours. After calcining, silver oxide was formed on cobalt sulfide and 0.1 M glucose was added to the composite to reduce silver. (Fig 2)

6. Methylene Blue Degradation Tests

In the degradation tests, 200 ml of a 10 mg/L MB solution was poured into the reactor. CoS was stirred for 90 minutes, during which samples were taken at various time intervals for spectrophotometric analysis. Silver was deposited onto CoS at different doping percentages (2% and 4%). The percentage of degradation was calculated using equation 1:

$$\text{Degradation}\% = \frac{C_0 - C_t}{C_0} \times 100 \quad (1)$$

Where:

C_0 is the initial and C_t is the concentration at time t.

7. Photolysis

To assess the effect of visible light irradiation on MB without the using catalyst, a 15 mg/L MB solution was prepared. The solution was exposed to visible LED light for 60 minutes without any catalyst present to evaluate the bleaching effect of light alone.

8. Adsorption on catalyst surface

To study the adsorption capacity of the silver-doped cobalt sulfide composite, an experiment was conducted in the absence of visible light. A 10 mg/L methylene blue solution was stirred magnetically in complete darkness for 60 minutes to assess adsorption behavior without light influence.

9. Investigating the Effect of pH

Based on prior research on cobalt sulfide adsorption at varying pH levels[48,49], experiments were conducted at pH values of 9, 7, and 4. The tests were carried out at a constant temperature of 30°C, using 0.4 g of catalyst for every 10 mg/L of methylene blue. For the purpose of isothermic investigations, a volume of 200 ml of methylene blue solution at differing concentrations (4, 6, 8, 10, 12 mg/L) incorporating 0.4 g of the composite was subjected to illumination from LED light within a cylindrical reactor.

10. Discussion & Conclusion

10.1. Interpretation of diffraction pattern

The X-ray diffraction analysis was performed to elucidate the composition and crystalline architecture of the synthesized specimen. The diffraction maxima detected at 2θ angles of 29.9°, 34°, 47.1°, and 56° are attributable to the (100), (101), (102), and (110) crystallographic planes of cobalt sulfide (CoS), respectively. Additionally, the peaks detected at specific 2θ values for silver are associated with the (111), (200), (220), and (311) planes (see Fig 2).

10.2. Calculating Crystallite Size Using the Williamson-Hall Method

To determine the strain and crystallite size using X-ray diffraction data, peak information was extracted using Expert High Score software. Subsequently, the corresponding curves were plotted using Excel software to analyze the crystallite size. (Fig 3)

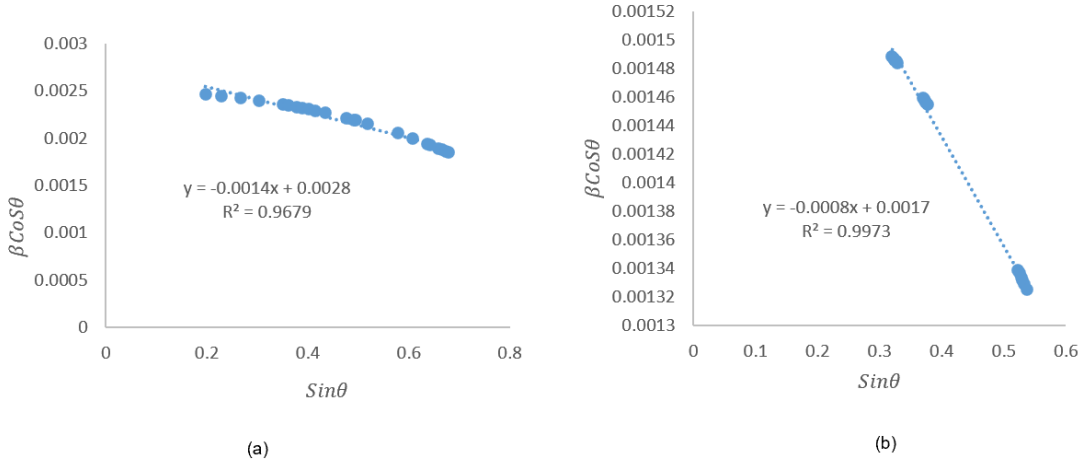

Figure 3. The β CoS versus θ curve plotted against sin θ is presented for calculating the crystallite size of (A) CoS and (B) Ag

$$\beta CoS\theta = \frac{K\lambda}{D} + 4\mathcal{E}\, Sin\theta \qquad (2)$$

In this particular context, D denotes the size of the crystallite measured in nanometers (nm), K represents a constant applicable to spherical particles (0.94), λ signifies the wavelength of the X-ray (Cu-Kα = 0.1541 nm), β corresponds to the peak width at half maximum height (FWHM), and θ indicates the angle of diffraction.

10.3. SEM and EDS results for CoS

Fig 4 displays scanning electron microscopy (SEM) images of the synthesized cobalt sulfide, captured at magnifications of 200 nm, 1 µm, and 500 nm. The morphology and size of the nanoparticles were influenced by the synthesis conditions, including temperature, reaction time, and pH. The EDS analysis showed that the composition of the nanoparticles consisted of cobalt and sulfur, with weight percentages of 60.2% and 39.8%, respectively.

10.4. SEM and EDS results for Ag/CoS Composite

Fig 5 presents the scanning electron microscopy (SEM) results for the synthesized Ag/CoS composite. The images were captured at magnifications of 200 nm, 500 nm, and 1 µm. The morphology reveals rectangular and polygonal structures, clearly indicating that cobalt sulfide and silver are effectively layered upon one another. The EDS analysis indicated that the composite is composed of cobalt, sulfur, and silver, with weight percentages of 63.1%, 31.9 %, and 5%, respectively.

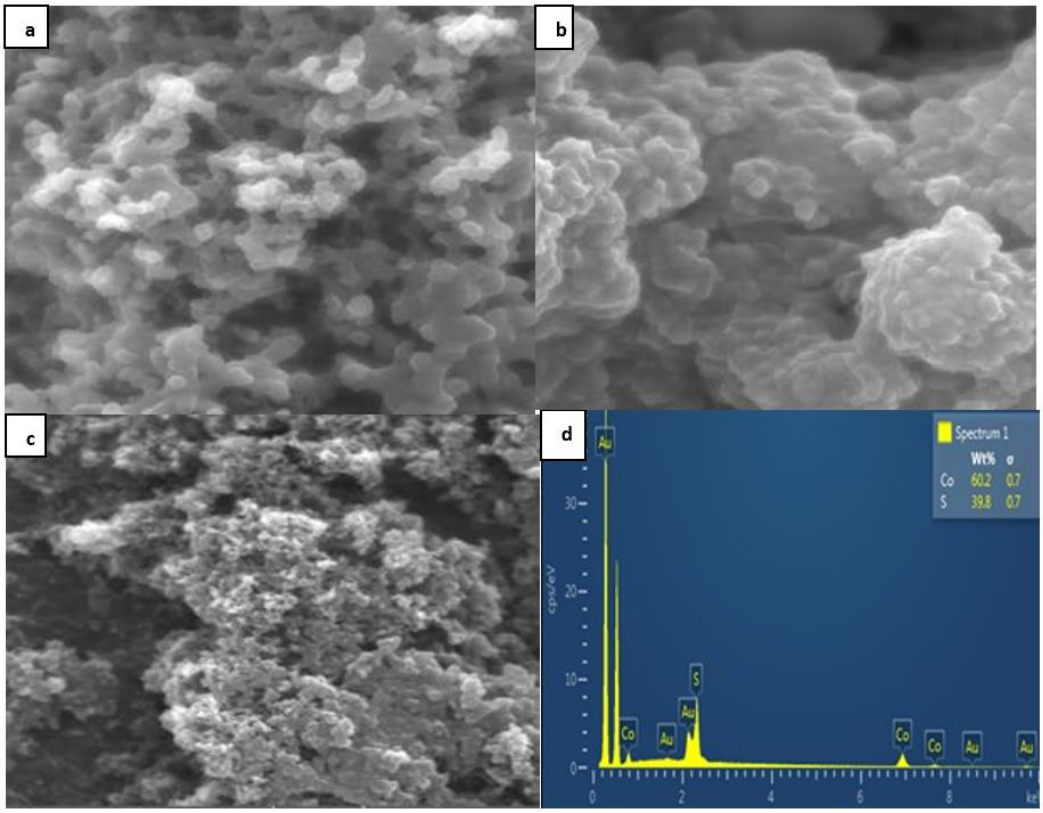

Figure 4. SEM images cobalt sulfide nanoparticles a) 200nm, b) 500nm, C) 1mm, d)EDS result

10.5. Band Gap Determination for CoS and Ag/CoS Composite

To determine the band gap of cobalt sulfide, the Kubelka-Munk method was employed:

$$\left[\frac{(1-R_\infty)^2}{2R_\infty} \times h\upsilon\right]^n = A(h\upsilon - E_g) \qquad (3)$$

Where A = Constant related to the material, hn = Photon energy, Eg = Optical bandgap, n = Exponent that depends on the nature of the electronic transition (n=1/2 for direct allowed transitions and n=2 for indirect allowed transitions). Fig 6 illustrates the cobalt sulfide bond, with the diagram expressed as $F(R) = (1-R)^2 / 2R$ in terms of energy (E in eV). From this diagram, the band gap for cobalt sulfide was found to be 2.6 eV, while for silver, it was determined to be 3 eV. The same method was applied to ascertain the band gap of the Ag/CoS composite, yielding a band gap of approximately 2.4 eV

10.6. Mott–Schottky Analysis

Mott-Schottky analysis is utilized to identify the semiconductor type and determine the flat band potential. The relationship is described by the equation:

$$\frac{1}{C^2} = 2(N_D \varepsilon \varepsilon_0)^{-1} \times \left(E - E_{fb} - {}^{kT}/_{e}\right) \qquad (4)$$

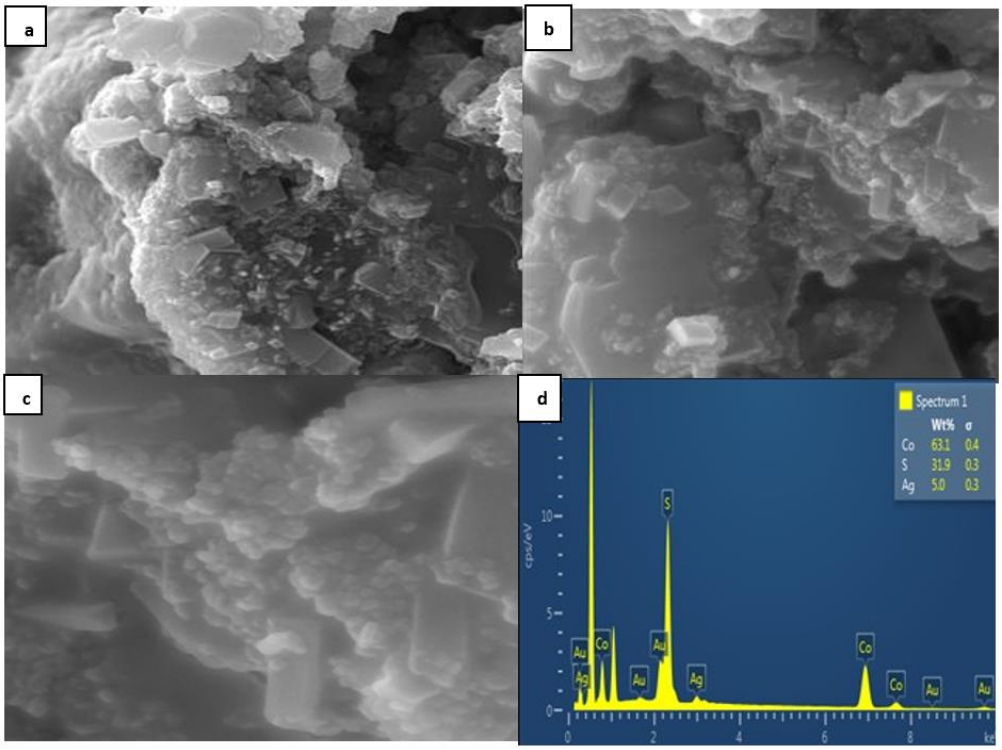

Figure 5. SEM images of a) 200nm, b) 500nm, c) 2µm, d) EDS results of Ag/CoS

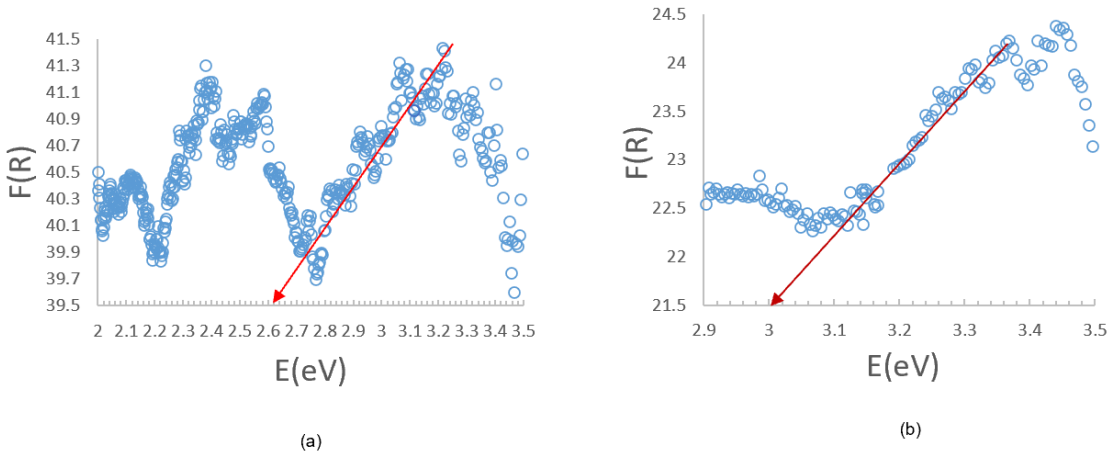

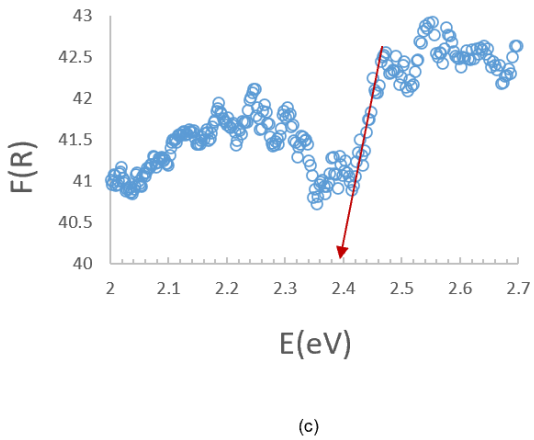

Figure 6. a) Cobalt sulfide bondage diagram. b) Silver Gap diagram c) Composite Gap diagram

In the aforementioned equation, C denotes the electric potential associated with the space charge, Ɛ signifies the dielectric constant inherent to the semiconductor, ND refers to the density of charge carriers, E represents the charge of an electron, Ɛ₀ indicates the permittivity of free space, E represents the applied electrode potential, Efb connotes the flat band potential, k is identified as the Boltzmann constant, and T represents the absolute temperature [50]. The Mott-Schottky plots corresponding to CoS and the Ag/CoS composite were generated by graphing $1/C^2$ in relation to the potential.

10.6.1. *Analysis of Mott–Schottky Results*

As presented in Fig 7, the positive slope observed in the Mott-Schottky diagram for the n-type semiconductor cobalt sulfide confirms the similar positive slope for the p-type silver semiconductor. The surface bond potential for cobalt sulfide (V) was measured at -1.2 V. The relationship for the reference electrode is given by [51]:

$$E_{NHE} = E_{\frac{Ag}{AgCl}} + .197\,V(PH = 7) \quad (5)$$

For cobalt sulfide, the flat band potential Efb relative to NHE is -1 V, while for silver, it is 1.69 V. Generally, the conduction band position of an n-type semiconductor is approximately 0.1 V lower than its Efb, whereas that of a p-type semiconductor is about 0.1 V higher than its Efb [52].

The valence band (EVB) values for cobalt sulfide and silver were calculated to be 1.5 V and 1.21 V, respectively. The energy band gap is defined by the equation:

$$E_g = E_{VB} - E_{CB} \quad (6)$$

where ECB represents the conduction band potential and EVB refers to the valence band potential [53]. Fig 8 provides a schematic representation of the Ag/CoS heterojunction.

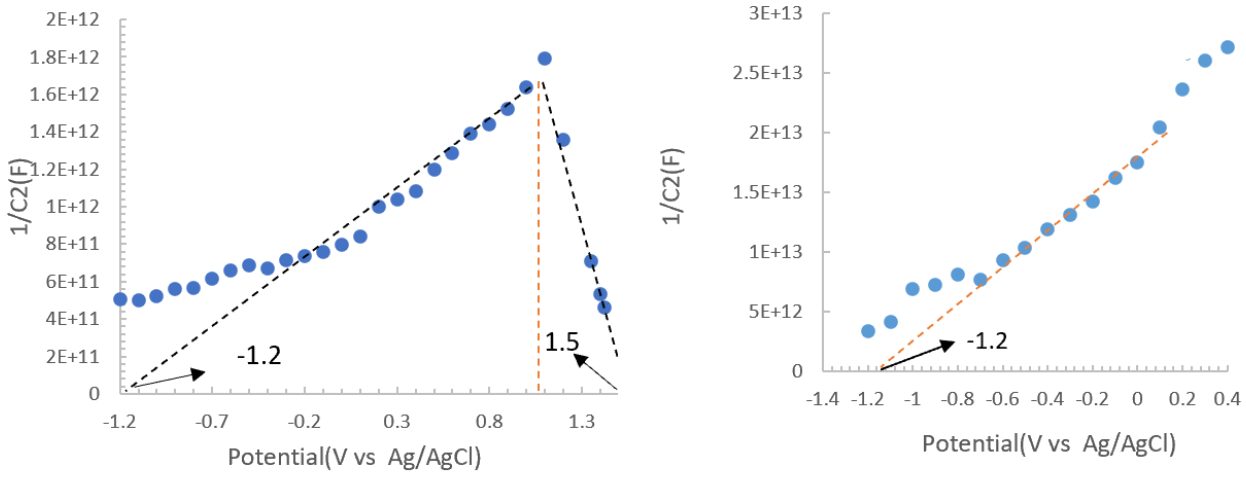

Figure 7. Matt-Schottky analysis for a)CoS b) Ag/CoS

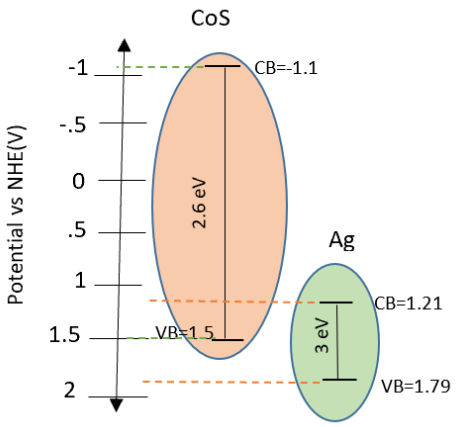

Figure 8. Schematic view of Ag/Cos heterojunction

11. Isothermic Studies

The preliminary phase in the majority of catalytic reactions entails the adsorption of the catalyst on the surface. In order to ascertain the most appropriate nonlinear isotherm model predicated on the minimization of error, a variety of isothermic models were utilized. This interval was regarded as the time required to achieve equilibrium. The ultimate concentration of the contaminant was quantified utilizing spectrophotometric technique. The equilibrium adsorption capacity was determined by equation (7):

$$q_e = \frac{(C_0 - C_e)V}{m} \quad (7)$$

In the aforementioned equation, C0 and Ce signify the initial and final concentrations (mg/L), respectively; V denotes the volume of the solution (L); m refers to the catalyst mass (g); and qe represents the mass of the pollutant absorbed per unit mass of the adsorbent (mg/g). The correlation coefficient (R^2) and corresponding error functions were employed to evaluate the thermodynamic behavior of the reactions across all isotherm models. In order to assess the degree of conformity of the laboratory data to the isotherm equations, MATLAB ® was utilized for the purpose of error minimization to calculate the statistical parameters pertinent to the aforementioned models, including the average relative error (ARE) and Marquardt's percentage standard deviation (MPSD) as two forms of error functions. Tables 1 and 2 delineate the relevant error functions and the resultant data obtained.

The Sips and Khan models exhibited the highest correlation coefficients alongside the lowest error functions, thereby substantiating their suitability as the most appropriate models for characterizing the adsorption process.

Table 1 Explanation of various error functions

Error Function	Abbreviation	
Average relative Error Function	ARE	$100\sqrt{\frac{1}{n-p}\sum_{i=1}^{n}\left(\frac{q_{e,\exp}-q_{e,\mathrm{cal}}}{q_{e,\exp}}\right)_i^2}$
Marquardt's percent The standard deviation error function	MPSD	$\frac{100}{n}\sum_{i=1}^{n}\left\lvert\frac{q_{e,\mathrm{cal}}-q_{e,\exp}}{q_{e,\exp}}\right\rvert_i$

Table 2. Nonlinear Isotherm Equations with Related Error Functions and Correlation Coefficient for Methylene Blue Adsorption Process Using Composite

Isotherm	Nonlinear form	Parameters (units)	Parameter values	R^2	ARE%	MPSD%
khan	$q_e=\frac{q_s,b_K,C_e}{(1+b_K,C_e)^{a_K}}$	q_s b_k a_k	0.055 6.768 -0.442	0.982	0. 078	0.01
Freundlich	$q_e=k_f,C_e^{1/n}$	kf n	0.915 0.704	0.915	0.0127	0.031
Sips	$q_e=\frac{k_s,a_s,C_e^{B_s}}{1+a_s,C_e^{B_s}}$	K_s α_S B_S	6.97 0.1 2.56	0.986	0.057	0.008
Radke_Prausnitz	$q_e=\frac{a_{RP},r_{RP},C_e}{1+r_{RP},C_e^{B_{RP}}}$	α_{RP} r_{RP} B_{RP}	0.04 29 -12	0.996	0.195	0.139

12. Reaction Kinetics and Thermodynamics

According to the results presented in Table 3 & 4, the Langmuir-Hinshelwood model exhibited a high correlation coefficient across various concentrations [54-59].

12.1.Reaction Kinetics and Thermodynamics

3 photocatalytic experiments were performed at temperatures of 30, 45, and 60 °C to determine thermodynamic parameters using Van't Hoff (Eq. 8) and Gibbs (Eq. 9) equations:

$$\ln K=-\frac{\Delta H^{\circ}}{R}\left(\frac{1}{T}\right)+\frac{\Delta S^{\circ}}{R} \quad (8)$$

$$\Delta G^{\circ}=\Delta H^{\circ}-T\Delta S^{\circ}=-RT\ln K \quad (9)$$

In these equations, ΔH° and ΔS° are the standard enthalpy change (kJ/mol) and standard entropy change (J/mol·K) respectively, K is the equilibrium constant, T is the absolute temperature in Kelvin, and R is the universal gas constant (8.3145 J/mol·K) [60]. The reaction equilibrium constant can be calculated using the following equation:

$$K = \frac{m}{v} \times \frac{q_e}{C_e} \quad (10)$$

where K is the reaction equilibrium constant, m is the catalyst mass (g), V is the total volume of the contaminant (L), qe is the amount of adsorbed contaminant per unit mass of adsorbent (mg/g), and Ce is the equilibrium concentration of the contaminant (mg/L). The activation energy for the process was determined using the Arrhenius equation:

$$ln\, k = -\frac{E_a}{RT} + ln\, A \quad (11)$$

where k is the rate constant (min^{-1}), Ea is the activation energy of the reaction (kJ/mol), R is the universal gas constant, A is the pre-exponential factor related to the probability of molecular collisions, and T is the temperature in Kelvin [61].

Table 5 provides additional details. According to the results presented in Table 5, the negative value of ΔH sugests that the photodegradation process is exothermic, while the negative value of ΔG indicates that the reaction is spontaneous within the temperature range of 30 to 60 °C.

Table 3. The Langmuir-Hinshelwood model

Heterogeneous catalysis kinetic model	Langmuir-Hinshelwood	$\frac{1}{k} = \frac{1}{K_{add}^{app} k_{L\cdot H}} + \frac{C_0}{k_{L\cdot H}}$

Table 4. Measured L-H parameters for photocatalytic reaction

Langmuir-Hinshelwood				
C_0 (mg/L)	$K\ (min^{-1})$	$k_{L\cdot H}$ (mg/L.min)	K_{add}^{app} (L/mg)	R^2
4	0.075			
6	0.074			
8	0.067	1.55	0.063	0.95
10	0.06			
12	0.055			

Table 5. Calculated thermodynamic parameters

ΔG°(k, J /mol)	ΔH°(kJ/mol)	ΔS°(J/mol.K)	E_a (kJ /mol)
-23.168	-10.292	40.489	2.52

13. Investigation of Methylene Blue photodegradation Under Different Conditions

The degradation of methylene blue using CoS was assessed at various time intervals. The optimal amount of silver was established by incorporating it into cobalt sulfide to form a composite. The degradation results for methylene blue are presented in Fig 9.The degradation percentage in visible light after 60 minutes was 1.45% without using a catalyst, indicating that photolysis had minimal impact on the degradation of methylene blue. Additionally, the degradation rate attributed to surface adsorption was reported to be 34% for methylene blue. In the experiments, the degradation rate of methylene blue using the composite at pH 9 was significant, while lower degradation rates were observed at pH levels 4 and 7. The performance of the catalyst synthesized in this study was compared to similar catalysts, as shown in Table 6. Furthermore, upon evaluating the adsorption phenomena of methylene blue subsequent to multiple utilizations of the catalyst, as delineated in Table 7, it can be inferred that the proportion of methylene blue adsorption diminishes with each instance of catalyst reapplication.

Table 6. Activity of Similar Photocatalysts in Methylene Blue Degradation

	Irradiation Source	Degradation efficiency	Reaction Time (min.)	Ref.
rGO@CoS	UV	100%	150	[62]
$CeO_2/Co_3O_4/Ag/Ag_3PO_4$	Visible	92.5%	80	[37]
CoS/Ag_2WO_4	Visible	91.8%	220	[43]
Ag/CoS	Visible	92%	15	This work

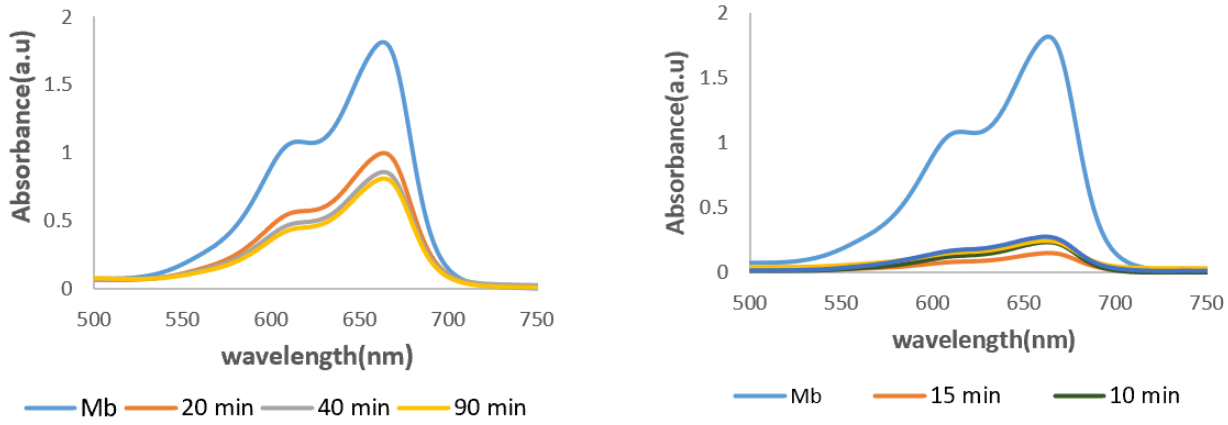

Figure 9. Absorbance vs. wavelength for degradation of MB on a) CoS b) Ag/CoS

Table 7. Methylene Blue degradation efficiency in consecutive cycles

Cycle No.	1	2	3	4	5
Degradation efficiency	92%	87%	75%	62%	52%

14. Conclusion

In conclusion, the Ag/CoS composite was successfully synthesized in a nanostructured form, achieving a degradation rate of 92% for methylene blue in just 15 minutes using 0.4 g of the composite in 200 ml of solution. Various isothermic models were employed to identify the best nonlinear model through error minimization. The Sips and Khan models exhibited the highest correlation coefficients and the lowest error functions, confirming their suitability for describing the adsorption process. Among the kinetic models, the Langmuir-Hinshelwood model showed the highest correlation coefficient. The bandgaps for cobalt sulfide, silver, and the composite were determined to be 2.6 eV, 3 eV, and 2.4 eV, respectively. The crystal sizes for cobalt sulfide and silver were found to be 49.5 nm and 79.81 nm. Additionally, the reaction was exothermic, and the negative ΔG value indicated that the reaction was spontaneous.

References

[1] P. Raizada, J. Kumari, P. Shandilya, P. Singh, Water Treat; 79 (2017) 204–213: https://doi.org/10.5004/dwt.2017.20831.

[2] R. Saravanan, M.M. Khan, V.K. Gupta, E. Mosquera, F. Gracia, V. Narayanan, A ,J. Colloid Interface; Volume 452, 15 August 2015, Pages 126-133: https://doi.org/10.1016/j.jcis.2015.04.035

[3] Rai HS, Singh S, Cheema PP, Bansal TK, Banerjee UC , Journal of environmental management; May 1;83(3)(2007):290-7: https://doi.org/10.1016/j.jenvman.2006.03.003

[4] Idrees Khan, Khalid Saeed, Ivar Zekker, Baoliang Zhang , Abdulmajeed H. Hendi, Ashfaq Ahmad, Shujaat Ahmad , Noor Zada, Hanif Ahmad, Luqman Ali Shah, Tariq Shah and Ibrahim Khan ,Water;(2022) 14, 242: https://doi.org/10.3390/w14020242

[5] Chun-Hsing Wu and Jia-Ming Chern. Ind. Eng. Chem. Res(2006);45, 6450-6457: https://doi.org/10.1021/ie0602759

[6] T.A. Saleh, V.K, Separ. Purif; Technol. 89 (2012) 245–251: https://doi.org/10.1016/j.seppur.2012.01.039

[7] R. Khaghani, B. Kakavandi, K. Ghadirinejad, E.D. Fard, A. Asadi ,Microporous Mesoporous Materials; 284(2019)111121:https://doi.org/10.1016/j.micromeso.2019.04.013

[8] I. Ali, M. Asim, T.A. Khan , Technol. 10 (2013) 377–384:https://doi.org/10.1007/s13762-012-0113-z.

[9] C.R. Klauck, M.A.S. Rodrigues, L.B. Silva ,Braz. J. Biol; 75 (2015) 57–62: https://doi.org/10.1590/1519-6984.1813

[10] M.R. Hoffman, S.T. Martin, W. Choi, D.W , Chem. Rev; 95 (1995) 69–96: https://doi.org/10.1021/cr00033a004

[11] Ladan Mohammadi , Reza Fazaeli , Zahra Khodadadi , J Photochem Photobiol A: https:// doi. org/ 10. 1016/j. jphot ochem. (2023). 114909

[12] Ladan Mohammadi , Zahra Khodadadi , Reza Fazaeli , Materials Chemistry and Physics; 1 February (2024), 128770: https://doi.org/10.1016/j.matchemphys.2023.128770

[13] Sai Bhargava Vuggili , Umesh Kumar Gaur , Tushar Tyagi and Manu Sharma ,Environ. Sci; 2(2023), 795-814: https://doi.org/10.1039/d2va00208f

[14] by Hui-Qi Chen,Jin-Ge Hao,Yu Wei,Wei-Ya Huang,Jia-Lin Zhang,Tao Deng,Kai YangandKang-Qiang Lu ,Catalysts; 13(3),(2023) 544: https://doi.org/10.3390/catal13030544

[15] Ta Cong Khiem , Xiaoguang Duan , Wei-Jie Liu , Young-Kwon Park , Ha Manh Bui , Wen-Da Oh , Suresh Ghotekar, Yiu Fai Tsang , Kun-Yi Andrew Lin , Chemical Engineering Journal; 453 (2023) 139699: https://doi.org/10.1016/j.cej.2022.139699

[16] Liu, Q.; Zhang, J. Y , CrystEngComm; 15 (2013) 5087−5092: https://doi.org/10.1039/c3ce40251g

[17] Du, G. H.; Li, W. Z.; Liu, Y. , J.Phys. Chem. C; 112(2008) 1890−1895:https://doi.org/10.1021/jp710543u

[18] Chen, X. Y.; Zhang, Z. J.; Qiu, Z. G.; Shi, C. W.; Li, X. L , J. Colloid Interface Sci; 308(2007) 271−275:https://doi.org/10.1016/j.jcis.2006.12.054

[19] Dong, W. J.; Wang, X. B.; Li, B. J.; Wang, L. N.; Chen, B. Y.; Li, C.R.; Li, X.; Zhang, T. R.; Shi, Z ,DaltonTrans 40(2011) 243−248: https://doi.org/10.1039/C0DT01107J

[20] Ramasamy, K.; Malik, M. A.; Raftery, J.; Tuna, F.; O'Brien, P , Chem. Mater; 22(2010) 4919−4930: https://doi.org/10.1021/cm1010345

[21] Yue, G. H.; Yan, P. X.; Fan, X. Y.; Wang, M. X.; Qu, D. M.; Wu, Z.G.; Li, C.; Yan, D ,Electrochem.SolidState Lett; 10(2007) D29−D31: https://doi.org/10.1149/1.2430564

[22] Wang, Q. H.; Jiao, L. F.; Du, H. M.; Peng, W. X.; Han, Y.; Song, D.W.; Si, Y. C.; Wang, Y. J.; Yuan, H. T, J. Mater. Chem; 21(2011) 327−329: https://doi.org/10.1039/C0JM03121F

[23] Wang, Y. M.; Wu, J. J.; Tang, Y. F.; Lü, X. J.; Yang, C. Y.; Qin, M.S.; Huang, F. Q.; Li, X.; Zhang, X, Mater. Interfaces; 4(2012)4246−4250: https://doi.org/10.1021/am300951f

[24] Gómez-Cámer, J. L.; Martin, F.; Morales, J.; Sánchez, J. Electrochem. Soc; 155(2008) A189−A195: https://doi.org/10.1149/1.2825137

[25] Pourahmad, A.; Sohrabnezhad, S.; Radaee, E , J. Porous Mater; 17(2010) 367−375: https://doi.org/10.1007/s10934-009-9301-8

[26] Sohrabnezhad,S.; Pourahmad, A.; Radaee, E,J. Hazard. Mater; 170(2009) 184−190: https://doi.org/10.1016/j.jhazmat.2009.04.108

[27] Panthi, G.; Barakat, N. A. M.; Khalil, K. A.; Yousef, A.; Jeon, K. S.; Kim, H. Ceram. Int; 39(2013) 1469−1476: https://doi.org/10.1016/j.ceramint.2012.07.091

[28] Zhao, C.; Li, D. Q.; Feng, Y. J , J. Mater.Chem.A; 1(2013) 5741−5746: https://doi.org/10.1039/C3TA10296C

[29] Sohrabnezhad, S , Spectrochim. Acta ; 81(2011) 228−235: https://doi.org/10.1016/j.saa.2011.05.109

[30] Wang, H. L.; Liang, Y. Y.; Li, Y. G.; Dai, H. J , Chem. Int. Ed.; 50(2011)1096910972: https://doi.org/10.1002/anie.201104004

[31] Zahra Alinezhad ,Reza Fazaeli, Hamidreza Moghadamzadeh, Mehdi Ardjmand , Nahid Raoufi, Catalysis Surveys from Asia.(2024):https://doi.org/10.1007/s10563-023-09420-z .

[32] Zhennan Xu , Junxiang Jiang , Qianqian Zhang , Dongmei Zhang a, Ling Li , Diamond & Related Materials; 116 (2021) 108448: https://doi.org/10.1016/j.diamond.2021.108448

[33] Junke Li, Mei li , Zhiliang Jin , Journal of Colloid and Interface Science; 592 (2021) 237–248: https://doi.org/10.1016/j.jcis.2021.02.053

[34] Hui-Qi Chen, Jin-Ge Hao, Yu Wei, Wei-Ya Huang , Jia-Lin Zhang , Tao Deng, Kai Yang and Kang-Qiang Lu ,Catalysts; 13(2023) 544: https://doi.org/10.3390/catal13030544

[35] Zhiliang Jin , Hongying Li , Junke Li , Chinese Journal of Catalysis 43(2022) 303–315: https://doi.org/10.1016/S1872-2067(21)63818-4

[36] G. Gurumoorthy, R. Hema.M. Sundararajan , Annals of R.S.C.B; ISSN:1583-6258, Vol. 25, Issue 2, 2021, Pages. 2086 – 2090: https://doi.org/10.26637/MJM0S200543

[37] Mohammad Mehdi Sabzehmeidani , Hajir Karimi , Mehrorang Ghaedi , Materials Research Bulletin; 147 (2022) 111629: https://doi.org/10.1016/j.materresbull.2021.111629

[38] M.I.A. Abdel Maksoud , Mohamed M. Ghobashy , Gharieb S. El-Sayyad , Ahmed M. ElKhawaga , Mohamed A. Elsayed ,A.H. Ashour ,Optical Materials; 119 (2021) 111396: https://doi.org/10.1016/j.optmat.2021.111396

[39] Maryam Farsi , Alireza Nezamzadeh-, Polyhedron ;219 (2022) 115823; https://doi.org/10.1016/j.poly.2022.115823

[40] S. Balasurya , Saleh Alfarraj , Lija L. Raju , Arunachalam Chinnathambi ,Sulaiman Ali Alharbi , Ajith M. Thomas , S. Sudheer Khan , Surfaces and Interfaces ;25 (2021) 101237: https://doi.org/10.1016/j.surfin.2021.101237

[41] Maryam Farsi , Alireza Nezamzadeh-Ejhieh , Surfaces and Interfaces; 32 (2022) 102148: https://doi.org/10.1016/j.surfin.2022.102148

[42] Qing Xu, Deli Jiang, Tianyong Wang, Suci Meng and Min Chen , RSC Adv; 6(2016) 55039–55045: https://doi.org/10.1039/C6RA08067G

[43] S. Kokilavani , Asad Syed , Hind A. AL-Shwaiman , Manal M. Alkhulaifi ,Fahad N. Almajdhi , Abdallah M. Elgorban , S. Sudheer Khan , Colloid and Interface Science Communications ; 42 (2021) 100415: https://doi.org/10.1016/j.colcom.2021.100415

[44] Huanli Wang, Lisha Zhang, Zhigang Chen, Junqing Hu, Shijie Li, Zhaohui Wang,Jianshe Liu and Xinchen Wang , Chem. Soc. Rev; 43(2014)5234—5244:https://doi.org/10.1039/C4CS00126E

[45] Jingxiang Low, Jiaguo Yu, Mietek Jaroniec, Swelm Wageh, and Ahmed A. Al-Ghamdi , Adv. Mater;(2017) 1601694: https://doi.org/10.1002/adma.201601694

[46] Zongpeng Wang , Zhiping Lin , Shijie Shen , Wenwu Zhong , Shaowen Cao , Chinese Journal of Catalysis ; 42(2021)710–730: https://doi.org/10.1016/S1872-2067(20)63698-1

[47] Hua Yang , Materials Research Bulletin; 142 (2021) 111406: https://doi.org/10.1016/j.materresbull.2021.111406

[48] S.M.R. Bavar, S. Alamolhoda, M. Sh Bafghi, S.M. Masoudpanah ,Journal of Physics and Chemistry of Solids(2022): https://doi.org/10.1016/j.jpcs.2020.109805

[49] Sajjad M. Flihh, Saad H , Environmental Nanotechnology, Monitoring & Management; 16 (2021) 100595: https://doi.org/10.1016/j.enmm.2021.100595

[50] Jin, X., Ye, L., Wang, H., Su, Y., Xie, H, Zhong, Z. and Zhang, H , B:Environmental;165(2015),pp.668-675: https://doi.org/10.1016/j.apcatb.2014.10.075

[51] Wen-Wen Dong , Jing Jia , Ye Wang , Jun-Rong An , Ou-Yang Yang , Xue-Jing Gao , Yun-Ling Liu , Jun Zhao, Dong-Sheng Li , Chemical Engineering Journal;438 (2022) 135622: https://doi.org/10.1016/j.cej.2022.135622

[52] Zhang, X., Tian, F., Lan, X., Liu, Y., Yang, W., Zhang, J. and Yu, Y , Chemical Engineering Journal; 429, p.132588(2022):https://doi.org/10.1016/j.cej.2021.132588

[53] Cao, Y., Alsharif, S. and El-Shafay, A.S , Materials Science in Semiconductor Processing; 144, p.106569(2022):https://doi.org/10.1016/j.mssp.2022.106569

[54] Saadi, Reyhaneh, Zahra Saadi, Reza Fazaeli, and Narges Elmi Fard ,Korean Journal of Chemical Engineering;32(2015):787-799: https://doi.org/10.1007/s11814-015-0053-7

[55] Jahromi, Leila Nassaji, Reza Fazaeli, Reza Behjatmanesh-Ardakani, and Mehdi Taghdiri , Journal of Photochemistry and Photobiology A: Chemistry;392 (2020): 112425: https://doi.org/10.1016/j.jphotochem.2020.112425.

[56] Fard, Narges Elmi, Reza Fazaeli, and Reza Ghiasi , Chemical Engineering & Technology;39, no. 1 (2016): 149-157:https://doi.org/10.1002/ceat.201500116

[57] Ehsan Ghorbannezhad, Susan Khosroyar, Farzad Kaj, International Journal Industrial Chemistry(IJIC)14(2023) -142301: https://dx.doi.org/10.57647/j.ijic.2023.1401.01

[58] Chunying Ba,International Journal Industrial Chemistry (IJIC)14(2023) -142305: https://dx.doi.org/10.57647/j.ijic.2023.1402.05

[59] Nassaji-Jahromi, Leila, Reza Fazaeli, Reza Behjatmanesh-Ardakani, and Mehdi Taghdiri ,Journal of the Chilean Chemical Society;65, no. 4 (2020): 5027-5034: http://dx.doi.org/10.4067/S0717-97072020000405027

[60] Saadi, Zahra, Reza Fazaeli, Leila Vafajoo, Iraj Naser, and Ghodratollah Mohammadi ,Chemical Engineering Communications;208, no. 3 (2021): 328-348:https://doi.org/10.1080/00986445.2020.1715955

[61] Park, Ju-Young, Kyung-Jun Hwang, Jae-Wook Lee, and In-Hwa Lee ,Journal of materials science; 46 (2011): 7240-7246: https://doi.org/10.1007/s10853-011-5683-5

[62] Anwaraporn Suramitr , Songwut Suramitr , Chayada Homhual , Natthakarn Saensanar ,Yingyot Poo-arporn , Narong Chanlek , Rungtiva P. Poo-arporn , Thin Solid Films;741 (2022) 139041: https://doi.org/10.1016/j.tsf.2021.139041